

1997

Grand Tour-Part 2: Petrogenesis and Thermal Evolution of Deep Continental-Crust: The Record from the East Humboldt Range, Nevada


Allen J. McGrew

University of Dayton, amcgrew1@udayton.edu

Mark T. Peters

Woodward-Clyde Federal Services

Follow this and additional works at: https://ecommons.udayton.edu/geo_fac_pub

 Part of the [Geology Commons](#), [Geomorphology Commons](#), [Geophysics and Seismology Commons](#), [Glaciology Commons](#), [Hydrology Commons](#), [Other Environmental Sciences Commons](#), [Paleontology Commons](#), [Sedimentology Commons](#), [Soil Science Commons](#), [Stratigraphy Commons](#), and the [Tectonics and Structure Commons](#)

eCommons Citation

McGrew, Allen J. and Peters, Mark T., "Grand Tour-Part 2: Petrogenesis and Thermal Evolution of Deep Continental-Crust: The Record from the East Humboldt Range, Nevada" (1997). *Geology Faculty Publications*. 40.
https://ecommons.udayton.edu/geo_fac_pub/40

This Article is brought to you for free and open access by the Department of Geology at eCommons. It has been accepted for inclusion in Geology Faculty Publications by an authorized administrator of eCommons. For more information, please contact frice1@udayton.edu, mschlangen1@udayton.edu.

Grand Tour—Part 2: Petrogenesis and thermal evolution of deep continental crust: the record from the East Humboldt Range, Nevada

ALLEN J. MCGREW

Department of Geology, The University of Dayton, Dayton, Ohio 45469-2364

MARK T. PETERS

Woodward-Clyde Federal Services, 1180 Town Center Drive, Las Vegas, Nevada 89134

INTRODUCTION

The northern part of the East Humboldt Range, Nevada, provides a rare opportunity to explore the petrogenetic environment of deep levels in the middle crust during both large-scale Mesozoic contraction and Cenozoic regional extension. On this segment of the field trip, we will explore evidence bearing on the character of the metamorphic and magmatic history of this terrane, and attempt to link these constraints to the rheology and tectonic evolution of the middle crust during the Mesozoic and Cenozoic.

TECTONIC SETTING

The northern East Humboldt Range forms the northernmost and perhaps the deepest seated part of the footwall of the Ruby Mountains–East Humboldt Range metamorphic core complex (Fig. 1). The western flank of the range forms a dip-slope on a gently inclined, normal-sense mylonitic shear zone at least 1 km thick, whereas the eastern flank of the range is bounded by a younger, steep east-dipping range-front normal fault that cuts through the metamorphic core complex to expose a spectacular natural cross-section (Figs. 10 and 11). Like other parts of the Ruby Mountains–East Humboldt Range, the northern East Humboldt Range records a complicated, polyphase history beginning with tectonic deep burial before the Late Cretaceous followed by deep-crustal tectonism during the Late Cretaceous to Oligocene and tectonic exhumation during Oligocene to early Miocene time. An important contrast between the northern East Humboldt Range and other parts of the Ruby Mountains–East Humboldt Range is that it exposes the only known outcrops of Archean rocks in the State of Nevada. Based on U-Pb geochronology and Sr, Nd, and Pb isotopic geochemistry, Wright and Snoke (1993) argue that the East Humboldt Range and Ruby Mountains are underlain by contrasting

crustal basement provinces of Archean and Proterozoic age, respectively (Fig. 1).

The structural architecture of the northern East Humboldt Range is dominated by two kilometer-scale features: a large, southward-closing, basement-cored recumbent fold known as the Winchell Lake fold-nappe, and the >1-kilometer thick mylonitic shear zone referred to above (Figs. 10 and 11) (Snoke and Lush, 1984; McGrew, 1992). We present evidence that the Winchell Lake fold-nappe was emplaced originally during the Late Cretaceous but was later transposed during Tertiary mylonitic shearing. An Archean orthogneiss occupies the core of the Winchell Lake fold-nappe and is surrounded by probable Paleoproterozoic paragneiss (Lush et al., 1988). Folded around this Precambrian gneiss complex, and separated from it by an inferred pre-folding, premetamorphic fault, is a metasedimentary sequence of quartzite, schist, and marble that probably correlates with the Neoproterozoic to Mississippian (?) miogeoclinal sequence of the eastern Great Basin. The inferred Paleozoic marble sequence repeats twice more at depth beneath the Winchell Lake fold-nappe, with a thick sequence of probable Neoproterozoic paragneiss intervening (see fig. 7B in Camilleri et al., this volume) (McGrew, 1992; Peters et al., 1992; Wickham and Peters, 1993). Inferred premetamorphic tectonic contacts bound each major package of rocks, and a thick sheet of hornblende-biotite quartz dioritic orthogneiss dated at 40 ± 3 Ma (U-Pb zircon, Wright and Snoke, 1993, RM-19) cuts gently across the various allochthons, including the tectonic slide at the base of the Winchell Lake fold-nappe. Numerous intrusions of biotite monzogranitic orthogneiss which are part of a widespread 29-Ma suite of dikes and sheets also cut the various allochthons, but are partially involved in folding and extensively overprinted by the mylonitic deformation (McGrew, 1992; Wright and Snoke, 1993). Taken together, the East Humboldt Range forms a stacked sequence of allochthons assembled during a complex,

polyphase tectonic history. A portion of the same stacked structural sequence is exposed east of the northern East Humboldt Range in the "Clover Hill" area (Snoke, 1992).

PRESSURE-TEMPERATURE HISTORY

Developing a pressure-temperature-time history (PTt path) for the East Humboldt Range depends critically on integrating quantitative thermobarometry with available cooling age constraints from radiometric dating and with relative age constraints developed from interpretive petrography and careful field observation. Below we first discuss constraints on the pressure-temperature path based on traditional petrography, field relationships, and quantitative thermobarometry, and then we integrate time-temperature constraints developed from radiometric dating in order to synthesize a PTt-path for the northern East Humboldt Range from the Late Cretaceous to early Miocene.

Petrographic and thermobarometric constraints

The northern East Humboldt Range exposes a diverse suite of metamorphic rocks, including leucogranitic to dioritic orthogneiss, amphibolite, calcite and dolomite marble, calc-silicate paragneiss, pelitic schist, and quartzite. The strongest constraints on the PTt history of the northern East Humboldt Range come from pelitic schists and to a lesser extent from amphibolites and calc-silicate paragneisses. For convenience, in the discussion below we will adopt emplacement of the Winchell Lake fold-nappe as a benchmark for notation of relative age relationships, designated by the subscript "n." Thus, M_n refer to metamorphism inferred to be synchronous with fold-nappe emplacement whereas M_{n-1} refers to metamorphic mineral growth predating fold-nappe emplacement, and M_{n+1} refers to metamorphic mineral growth postdating fold-nappe emplacement.

In general, metamorphic mineral assemblages show little geographic variation throughout the northern East Humboldt Range. However, the oldest phase in the metamorphic history of the northern East Humboldt Range is preserved only on the upper limb of the Winchell Lake fold-nappe where scarce subassemblages of kyanite \pm staurolite + biotite persist locally as inclusion suites in garnet. Kyanite also survives locally in the matrix of some pelitic schists where it is mantled or pseudomorphosed by later sillimanite. At present, the only constraint on the age of this kyanite-bearing subassemblage is that it must predate formation of the Winchell Lake fold-nappe because the sillimanite that replaces it is itself pre- to early synkinematic with fold-nappe emplacement. However, by analogy with similar assemblages in the Wood Hills and Clover Hill to the east, we suggest that the kyanite-bearing assemblages (M_{n-1}) in the northern East Humboldt Range prob-

ably record tectonic burial in the Late Jurassic and/or Early Cretaceous (Hodges et al., 1992; Snoke, 1992; Camilleri and Chamberlain, 1997).

The characteristic peak metamorphic assemblage in pelitic schists consists of biotite + sillimanite + garnet + quartz + plagioclase \pm K-feldspar \pm muscovite \pm chlorite \pm rutile \pm ilmenite. In a few samples from deep structural levels, sillimanite and metamorphic potassium feldspar coexist in rocks that are nearly devoid of muscovite, suggesting that peak metamorphism may have reached the second sillimanite isograd. As noted above, much of the sillimanite shows textural relationships that are pre- or early synkinematic relative to emplacement of the Winchell Lake fold-nappe, and therefore pre-kinematic with respect to the later extensional shearing. For example, mats of sillimanite are folded in the hinge zone of the Winchell Lake fold-nappe, and in the mylonitic zone bundles of sillimanite are commonly boudinaged, deflected by extensional crenulation cleavage, or cut by microfractures oriented perpendicular to Tertiary stretching lineation. Below we argue that this initial phase of sillimanite growth occurred synchronously with fold-nappe emplacement (M_n) and was Late Cretaceous. Nevertheless, textural relationships commonly record more than one phase of sillimanite growth, and the final phase of sillimanite growth (M_{n+1}) probably occurred during Oligocene extensional deformation. For example, fine-grained intergrowths of dynamically recrystallized quartz, fibrolite, and biotite occur along some extensional shear bands.

Many shear band fabrics and extensional microfractures also contain relatively late-stage minerals (M_{n+2}) such as chlorite and muscovite, demonstrating that mylonitic deformation continued through a range of progressively lower grade conditions during extensional exhumation. Although muscovite occurs at all structural levels, overprinting of earlier fabrics and assemblages by coarse, patchy muscovite becomes increasingly conspicuous at higher levels in the mylonitic shear zone.

The assemblages described above are amenable to quantitative thermobarometry based on electron microprobe analysis using the Thermocalc computer program of Powell and Holland (1988) and the internally consistent thermodynamic data set of Holland and Powell (1990). P-T estimates obtained by this method define a linear trend from approximately 8.7 kb, 790°C to 2 kb, 540°C (Fig. 20) (Hurlow et al., 1991; Hodges et al., 1992; McGrew and Peters, unpublished data). We believe that this steeply inclined P-T trend records decompressional metamorphism that accompanied exhumation of the East Humboldt Range from the Late Cretaceous to late Oligocene (see below). The samples yielding the lowest P-T estimates (2–4.2 kb, 540°C–650°C) include minerals such as muscovite that grew synkinematically with extensional shear-

ing as part of the equilibrium assemblage (Hurlow et al., 1991; Hodges et al., 1992; McGrew and Peters, unpublished data). Accordingly, these results represent the best estimate for P–T conditions accompanying mylonitic deformation. In addition, because the closure temperature range for $^{40}\text{Ar}/^{39}\text{Ar}$ dating of hornblende (480°C–580°C) overlaps these P–T estimates, cooling ages of 26–32 Ma in the northern Ruby Mountains (Dallmeyer et al., 1986) and 29–36 Ma at deep structural levels in the East Humboldt Range (McGrew and Snee, 1994) probably record the approximate timing of this final stage of metamorphic equilibration (see below).

Metacarbonate and metabasite mineral parageneses are largely compatible with the results from pelitic schists reported above. For a discussion of calc-silicate phase equilibria see the section on metamorphic fluids below. Metabasite mineral assemblages most commonly occur in small amphibolite bodies in the Paleoproterozoic and Archean gneiss sequences of Angel Lake near the northern end of the range. Characteristic assemblages commonly include amphibole + plagioclase ± biotite ± garnet ± quartz ± clinopyroxene ± ilmenite ± sphene ± magnetite ± rutile ± apatite ± chlorite. Many amphibolites contain moderately to severely resorbed garnet porphyroblasts surrounded by a symplectite of plagioclase ± hornblende ± biotite. This classic decompression texture lends additional support to the decompressional PTt-path outlined above. Depending on fluid activities, P–T results for the above assemblage range from 6.1 kb, 470°C for $a_{\text{H}_2\text{O}} = 0.1$ to 8.4 kb, 600°C for $a_{\text{H}_2\text{O}} = 1.0$ (Fig. 20) (McGrew and Peters, unpublished data). The temperature range for this sample corresponds quite closely with the closure temperature range for $^{40}\text{Ar}/^{39}\text{Ar}$ dating of hornblende, so an $^{40}\text{Ar}/^{39}\text{Ar}$ hornblende cooling age of 51.0 ± 2 Ma on a nearby amphibolite provides a plausible estimate for the timing of equilibration. The lower temperature of this P–T estimate as compared with pelitic assemblages raises the possibility that the amphibolite sample records a cooling event at this time that is not seen in the results from the metapelites.

Radiometric age constraints and an integrated PTt-path

A variety of radiometric age data including U–Pb, $^{40}\text{Ar}/^{39}\text{Ar}$, and fission-track data provide critical constraints on the timing of metamorphism in the East Humboldt Range. The key date constraining the timing of peak metamorphism (M_n) comes from a preliminary U–Pb, zircon age of 70–90 Ma (J. E. Wright, personal comm., 1992) on a small body of pegmatitic leucogranite collected in the hinge zone of the Winchell Lake fold-nappe. The leucogranite in question is clearly folded around the nose of the Winchell Lake fold-nappe, but larger-scale field relationships strongly suggest that it was emplaced synkinemati-

cally with the fold-nappe. It belongs to a suite of leucogranitic bodies that are strongly associated with a rusty-weathering, graphite-rich pelitic schist and paragneiss unit that forms a continuous, distinctive layer within the inferred Paleozoic miogeoclinal sequence on the upper limb of the Winchell Lake fold-nappe (McGrew, 1992). As this unit is traced into the hinge zone of the Winchell Lake fold-nappe, the volume percent of leucogranite increases gradationally but dramatically, from <25% to >65% over a distance of ~2 km. In addition, relict kyanite on the upper limb of the Winchell Lake fold-nappe occurs most commonly in this same unit, but it is completely replaced by sillimanite over this same interval. The volume percent of leucogranite in the weakly migmatitic marbles that surround these rocks show no systematic variations over this same interval. On the lower limb of the fold-nappe this same unit never exceeds 5 m in thickness, and in many localities it is completely absent or exists only as isolated rafts of graphitic, biotite-rich melanosome suspended in small bodies of leucogranite. Commonly, the leucogranite can be traced into the country rock where it forms small pods and seams intricately interdigitated with selvages of melanosome enriched in biotite, iron oxide, and graphite, suggesting an origin by localized partial melting. In any case, the observation that migmatitic layering clearly wraps around the fold hinge in combination with the fact that leucogranite isopleths cut the Winchell Lake fold-nappe, implies that leucogranite generation and emplacement was synkinematic to fold-nappe emplacement. Therefore, the Late Cretaceous U–Pb zircon age of 70–90 Ma referred to above probably dates both fold-nappe emplacement and a major syntectonic magmatic-metamorphic event (M_n). We suggest that the highest P–T results shown on Figure 20 (approximately 8.7 kb, 790°C) probably date from this time.

The thermal history of the East Humboldt Range following peak metamorphism in the Late Cretaceous depends mostly on $^{40}\text{Ar}/^{39}\text{Ar}$ and fission-track cooling age constraints summarized in Figure 21. Temperature estimates for pelitic assemblages in the northern half of the East Humboldt Range are all well above the nominal closure temperature range for $^{40}\text{Ar}/^{39}\text{Ar}$ dating of hornblende (480°C–580°C), and thus $^{40}\text{Ar}/^{39}\text{Ar}$ hornblende cooling ages bracket the age of metamorphism. For samples collected above 9600 ft (2930 m) this age limit is defined by hornblende cooling ages between 50 and 63 Ma (McGrew and Snee, 1994). However, at lower elevations final cooling through $^{40}\text{Ar}/^{39}\text{Ar}$ hornblende closure temperatures did not occur until the early Oligocene (30–36 Ma), resulting in a much broader age bracket. Samples from higher structural levels yield P–T estimates in the range 6.4 to 8.7 kb, 635°C to 800°C (for $a_{\text{H}_2\text{O}} = 1.0$), whereas those from deeper structural levels range from 4.5 to 9.1 kb and

PT Results, East Humboldt Range

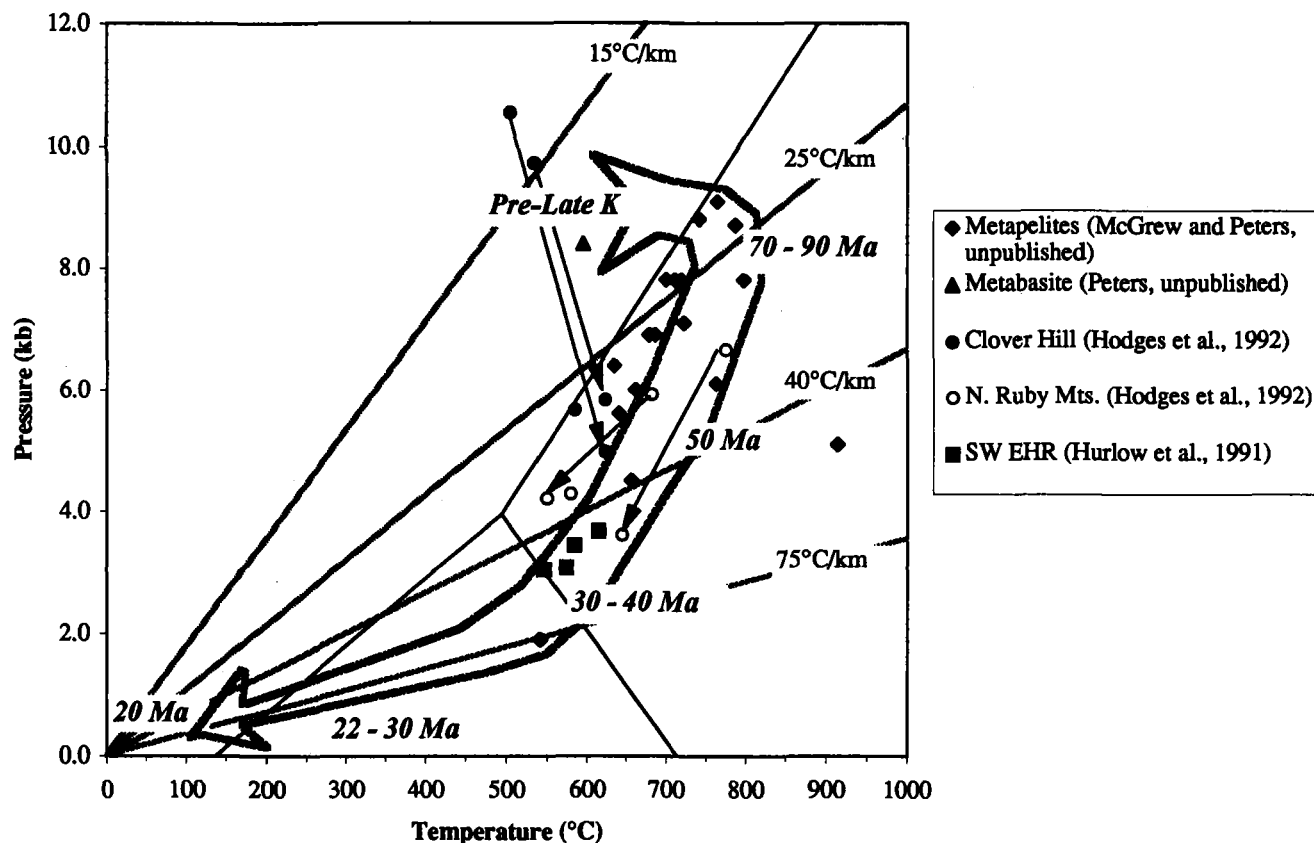


Figure 20. Synoptic diagram of P-T estimates from the central and northern East Humboldt Range determined by the authors using the updated, internally consistent thermodynamic data set of Holland and Powell (1990) and the Thermocalc computer program of Powell and Holland (1988) combined with previously published P-T results from elsewhere in the Ruby-East Humboldt metamorphic complex (Hurlow et al., 1991; Hodges et al., 1992). The large shaded arrow represents the general P-T path inferred for the East Humboldt Range for late Mesozoic time to ~20 Ma. The light arrows represent P-T paths based on Gibbs Method modeling of garnet zoning profiles reported in Hodges et al. (1992). Shaded lines provide reference geotherms of 15°C/km, 25°C/km, 40°C/km, and 75°C/km. The modern day geothermal gradient in the Basin and Range province is approximately 25°C/km, whereas the Battle Mountain heat flow high is characterized by geothermal gradients on the order of 40–75°C/km (Lachenbruch and Sass, 1978). Stability fields for the Al_2SiO_5 polymorphs are also provided for reference (also calculated using the data of Holland and Powell [1990] and Powell and Holland [1988]).

640°C to 765°C (McGrew and Peters, unpublished data). The broader range in pressures recorded at deep levels suggests that the lower pressure samples were probably reset during reheating accompanying Oligocene extensional unroofing. In addition, one sample from the central part of the range yields a much lower pressure estimate of 2 kb, 540°C, and exhibits textural relationships that strongly imply that it reequilibrated during extensional shearing. This sample was collected at approximately the level of the transition between the younger and older hornblende cooling ages, so an Oligocene age for final equilibration is plausible (Hurlow et al., 1991; McGrew and Peters, unpublished data). Important implications of

this history are that the northern East Humboldt Range must have experienced ≥ 20 km of unroofing before it experienced dramatic cooling, and that over 7 km (> 2 kb) of this unroofing may have occurred before middle Eocene time. This lends credence to previously published suggestions that extensional unroofing in northeastern Nevada began as early as Eocene or even Late Cretaceous time (Hodges et al., 1992; McGrew and Snee, 1994; Camilleri and Chamberlain, 1997).

Following cooling through $^{40}\text{Ar}/^{39}\text{Ar}$ hornblende closure temperatures (480°C–580°C), the cooling history of the northern East Humboldt Range is constrained mostly by $^{40}\text{Ar}/^{39}\text{Ar}$ mica and fission-track apatite cooling ages

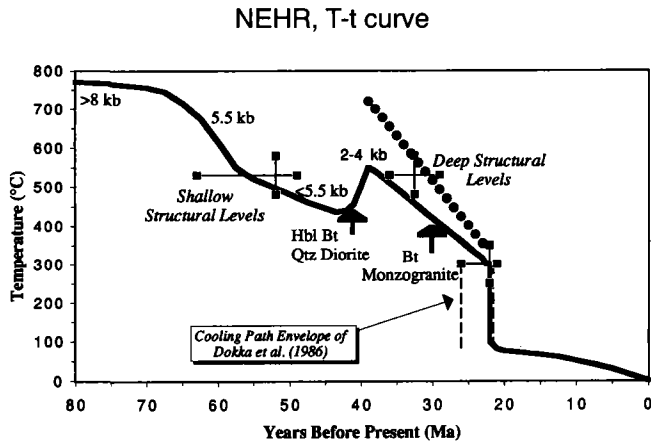


Figure 21. A proposed time-temperature history for the northern East Humboldt Range from the Late Cretaceous to Present, integrating the $^{40}\text{Ar}/^{39}\text{Ar}$ results of McGrew and Snee (1994) with older thermochronometric results (Dallmeyer et al., 1986; Dokka et al., 1986). Pressure estimates are also included, based on integration of P-T results reported by McGrew (1992), Peters (1992), and Hurlow et al. (1991) (see also Fig. 20). The solid curve represents relatively shallow structural levels (and thus also a lower temperature bound for relatively deep structural levels), whereas the dotted curve represents an upper temperature bound for relatively deep structural levels. Heavy arrows denote important igneous events: (a) intrusion of the hornblende-biotite quartz dioritic orthogneiss sheet at 40 ± 3 Ma and eruption of andesitic to rhyolitic tuffs; and (b) intrusion of biotite monzogranitic dikes and sheets at 29 ± 0.5 Ma (Wright and Snoke, 1993). We favor a distinct thermal pulse at the time of quartz dioritic intrusion and widespread ignimbrite eruption (~ 40 Ma), but we cannot rule out the alternative interpretation of gradual slow cooling from ~ 50 Ma to ~ 30 Ma.

(Dallmeyer et al., 1986; Dokka et al., 1986; McGrew and Snee, 1994). In any given area $^{40}\text{Ar}/^{39}\text{Ar}$ muscovite and biotite cooling ages are identical to each other and to fission-track apatite cooling ages within analytical uncertainties, thus implying cooling rates on the order of $100^\circ\text{C}/\text{m.y.}$ in the northern part of the range during the late Oligocene and early Miocene (Fig. 21) (Dokka et al., 1986; McGrew and Snee, 1994). In addition, $^{40}\text{Ar}/^{39}\text{Ar}$ mica cooling ages document diachronous cooling of the East Humboldt Range through $^{40}\text{Ar}/^{39}\text{Ar}$ biotite closure temperatures (250°C – 300°C), from ~ 32 Ma in the south to ~ 21 Ma in the north (Dallmeyer et al., 1986; McGrew and Snee, 1994). Moreover, geographic comparison of fission-track and mica cooling ages indicates that the southeastern part of the range had cooled through fission-track apatite closure temperatures ($\sim 110^\circ\text{C}$) while areas as little as 7 km to the west had not yet cooled through $^{40}\text{Ar}/^{39}\text{Ar}$ muscovite closure temperatures (300°C – 350°C). McGrew and Snee (1994)

show how these cooling age relationships could be explained by progressive rolling-hinge style unroofing of the footwall of a west-northwest-directed normal fault system.

METAMORPHIC FLUIDS: GEOCHEMISTRY, EVOLUTION, AND RELATIONSHIP TO LEUCOGRANITE PETROGENESIS

In this section we outline the relationship between fluid geochemistry and the metamorphic and magmatic evolution of the East Humboldt Range, with particular attention to the origin and significance of the abundant leucogranitic bodies that occur throughout the range. At relatively high structural levels throughout the northern half of the range, variations in leucogranite percentage are primarily controlled by the host lithology. Marbles and pure quartzites commonly contain $<10\%$ leucogranite, whereas pelitic or semi-pelitic units, impure metapsammitic rocks, and quartzo-feldspathic gneiss contain variable amounts of leucogranite, ranging from $<15\%$ to $>75\%$ by volume (McGrew, 1992).

At deeper structural levels, beneath the hornblende-biotite quartz diorite sill, leucogranite proportions in the paragneiss sequence of Lizzies Basin increase systematically and dramatically, from values generally $<50\%$ above 9400 ft (2865 m) to values $>65\%$ (locally $>90\%$) at elevations below 9000 ft. (2745 m) (see Fig. 7B in Camilleri et al., this volume) (McGrew, 1992; Peters and Wickham, 1995). Textural relationships, such as fine-scale interdigitations of leucosome and melanosome, suggest that some rocks represent in situ partial melts. However, the sheer volume of leucogranite suggests that a sizable fraction must have been externally-derived (Peters and Wickham, 1995). We refer to this sequence of extremely migmatitic rocks informally as the migmatite complex of Lizzies Basin, and we take the 65% leucogranite isopleth as its upper boundary, although it should be remembered that this boundary is actually gradational across a narrow interval. In addition, large, finger-like bodies of leucogranite originating from the Lizzies Basin migmatite complex locally penetrate upward into the overlying rocks. No age dates currently exist for the Lizzies Basin leucogranite suite, but we note that some of the leucogranitic bodies cut the 40-Ma quartz dioritic sill and 29-Ma monzogranitic sheets.

The roof of the migmatite complex of Lizzies Basin also coincides with an important oxygen isotope discontinuity (the contact between the lower zone and the upper zone in Figure 9) and with the nearly complete replacement of marble by calc-silicate rock below (Wickham and Peters, 1990; McGrew, 1992; Peters and Wickham, 1995). The metasedimentary rocks of the lower zone (i.e., the migmatite complex) exhibit uniformly low $\delta^{18}\text{O}$ values implying equilibration with a large, isotopically light fluid reser-

voir (see also Wickham and Peters, 1992; Wickham et al., 1993; Bickle et al., 1995). By contrast, the rocks of the upper zone show higher and generally more variable $\delta^{18}\text{O}$ values (Wickham and Peters, 1990; Peters and Wickham, 1995). Furthermore, all calc-silicate samples in the Lizzies Basin migmatite complex show extensive late-stage overgrowths of amphibole \pm epidote \pm garnet, suggesting a late-stage, high-temperature, H_2O -rich fluid infiltration event (Peters and Wickham, 1994). In addition, where this late-stage assemblage is well-developed at shallower structural levels it is generally associated with nearby leucogranites, further documenting the relationship between metasomatism and magmatism (Peters and Wickham, 1994; 1995). Finally, this late-stage assemblage occurs locally in extensional shear bands, pull-apart zones, or veins orthogonal to the extensional stretching lineation, suggesting a synextensional origin for both the migmatite complex of Lizzies Basin and the final episode of high-grade metamorphism.

SUMMARY AND CONCLUSIONS

The northern East Humboldt Range preserves a complex, evolving record of deep-crustal metamorphism, fluid infiltration, and anatexis during large-scale contractional and extensional tectonism from the late Mesozoic to early Miocene. Relict kyanite + staurolite assemblages record tectonic deep burial of the northern East Humboldt Range during the earliest stages of this history before the Late Cretaceous. Peak metamorphism occurred in the Late Cretaceous synkinematically with emplacement of a large, southward-closing recumbent fold-nappe, the Winchell Lake nappe. Peak metamorphism attained P–T conditions as high as 8.7 kb, 790°C, approaching or exceeding the second sillimanite isograd, and resulting in the generation and emplacement of abundant leucogranitic bodies. Primary assemblages in calc-silicate rocks may date from this time and indicate equilibration with an internally buffered(^p), CO_2 -rich pore fluid.

Following the Late Cretaceous the rocks experienced decompressional metamorphism through much of the Tertiary, with decompression of at least 2 kb (>7 km of unroofing) before approximately 50 Ma. Rocks at high

structural levels cooled through the closure temperature range for $^{40}\text{Ar}/^{39}\text{Ar}$ dating of hornblende (480°C–580°C) by ~50 Ma, but rocks at deeper structural levels did not finally close to argon diffusion in hornblende until early Oligocene time (30–36 Ma). During this time period, metamorphism at conditions of at least 2.0–4.2 kb, 540°C–650°C developed synkinematically with the early stages of west-northwest-directed extensional mylonitic deformation. However, fault rocks in the northern East Humboldt Range show a continuous ductile through brittle deformational evolution. In addition, $^{40}\text{Ar}/^{39}\text{Ar}$ mica and fission-track cooling age constraints indicate that the East Humboldt Range was ultimately exhumed by diachronous unroofing in the footwall of an evolving, west-rooted normal fault system from the late early Oligocene to early Miocene (Mueller and Snoke 1993a).

Secondary subassemblages of amphibole + epidote + garnet in calc-silicate rocks probably also grew during synextensional Oligocene metamorphism, recording intensive metasomatism by water-rich brines that probably came from crystallization of abundant leucogranitic bodies at deep structural levels. During this late stage, H_2O -rich fluid infiltration event metamorphic conditions probably evolved from early high temperature (600°C–750°C) to later, lower temperature conditions (<525°C). Pervasive fluid infiltration at deep structural levels produced wholesale reequilibration and homogenization of the oxygen isotope systematics to uniformly low values of $\delta^{18}\text{O}$. We suggest that the leucogranitic melts acted as a proxy, or vector of transport for fluids that ultimately derived from injection of mantle-derived basaltic magma at lower crustal levels. In contrast, rocks at higher structural levels show higher and more variable values of $\delta^{18}\text{O}$ that reflect the original sedimentary isotope systematics. If these conclusions are true, then much of the deep crust of northeastern Nevada may have been buffered at melting conditions during the primary phases of extensional tectonism and metamorphic core complex development. Consequently, we envision a deep-crustal environment that was rheologically weak and subject to asthenosphere-like flow on geologically reasonable time-scales.